The Cryosphere Discuss., 5, 479–498, 2011
www.the-cryosphere-discuss.net/5/479/2011/
doi:10.5194/tcd-5-479-2011

The Cryosphere Discussions

In-situ multispectral and bathymetric measurements over a supraglacial lake in western Greenland using a remotely controlled watercraft

M. Tedesco and N. Steiner

The City College of New York, The City University of New York, New York, 10031, NY, USA

The Graduate Center, The City University of New York, New York, 10016, NY, USA

Received: 31 December 2010 – Accepted: 19 January 2011 – Published: 7 February 2011

Correspondence to: M. Tedesco (mtedesco@sci.ccny.cuny.edu)

Published by Copernicus Publications on behalf of the European Geosciences Union.

Abstract

We report concurrent in-situ multi-spectral and depth measurements over a supraglacial lake in West Greenland, collected by means of a remotely controlled boat equipped with a GPS, a sonar and a spectrometer. We focus our attention on the analysis of some of the key parameters widely used for multispectral spaceborne bathymetry, namely the lake bottom albedo and the water attenuation coefficient. The analysis of in-situ data highlights the exponential trend of the water-leaving reflectance with lake depth. The values of the attenuation factor are obtained from in-situ data and compared with those computed using approaches proposed in the literature. Also, the values of the lake bottom albedo from in-situ measurements are compared with those obtained from the analysis of reflectance of shallow-waters. Finally, we quantify the error between in-situ measured and satellite-estimated lake depth values for the lake under study.

1 Background and rationale

Supraglacial lakes are pools of meltwater that form during summer in depressions in the ice sheet surface. Monitoring the spatio-temporal variability of such lakes over the Greenland ice sheet (GrIS) can benefit studies concerning ice sheet dynamics (Das et al., 2008; Joughin et al., 1996; Pimentel and Flowers, 2010) and surface features (e.g., Lüthje et al., 2006). Recently, several approaches based on the interpretation of visible and near-infrared satellite data have been proposed for estimating supraglacial lake depth (e.g., Georgiou et al., 2009; Box and Ski, 2007). McMillan et al. (2007) use satellite imagery to study the evolution of 292 lakes over an area of 22 000 km^2; Sundal et al. (2009) analyze 268 cloud-free Moderate Resolution Imaging Spectroradiometer (MODIS) images; Sneed and Hamilton (2007) estimate the depth of selected lakes based on Advanced Spaceborne Thermal Emission and Reflection radiometer (ASTER) atmospherically corrected reflectance values.

TCD
5, 479–498, 2011

Supraglacial lake depth can be estimated from visible reflectance measurements considering that the reflectance of a water column that is limited by a reflecting bottom is equal to the reflectance of the same water body in absence of a bottom plus the bottom contrast, after this contrast has been modulated by the depth of the bottom through an attenuation factor (Philpot, 1989; Maritorena, 1994). For retrieval purposes, the following hypotheses on the bottom albedo *Ad* and on the attenuation factor *g* are made: (Hyp. 1) in the absence of actual measurements the value of *Ad* is assumed to be uniform and (Hyp. 2) *Ad* is estimated from reflectance values of shallow waters along the lake edge (e.g., Sneed and Hamilton, 2007); the attenuation factor *g* is computed assuming that (Hyp. 3) suspended or dissolved organic or inorganic particulate matter is minimal and that (Hyp. 4) a linear relationship exists between the attenuation factor and the diffuse attenuation coefficient (e.g., Maritorena, 1994). Measurements of organic, chlorophyll and suspended minerals by Sneed and Hamilton (2007) confirmed that concentrations are appreciably small (less than $1\,\mathrm{mg\,L^{-1}}$). Similar concentrations were confirmed by our analysis of water samples collected from different lakes. Though spectrally similar to the diffuse attenuation coefficient for downwelling light *Kd*, *g* and *Kd* cannot be used interchangeably and a possible range of $1.5\,Kd < g < 3\,Kd$ is suggested by Philpot (1989) in the case of strongly absorbing waters. The value of $g \approx \alpha \cdot Kd$ with $\alpha = 2$ has been used by Sneed and Hamilton (2007) and Maritorena et al. (1994), with the latter warning that such a choice will lead to an unquantifiable underestimation of the actual attenuation.

Focusing on the bottom albedo *Ad*, Sneed and Hamilton (2007) and Georgiou et al. (2009) suggest that the uncertainty deriving from the selection of *Ad* is the highest. As said, for this parameter the assumption of uniform distribution over the lake is used for retrieval purposes and its value is estimated by searching for pixels adjacent to those showing a rapid decrease in the red band (Sneed and Hamilton, 2007). In other words, because of the relatively small attenuation in the green and blue bands with respect to the red band, the bottom albedo Adis assumed to be spectrally similar to the pixels where water is shallow, at the edge of the lake.

TCD
5, 479–498, 2011

The assumptions applied to the estimation of *Ad* and the choice of α are a source of uncertainty on the accuracy of lake depth retrieval from spaceborne data. Here we report, for the first time, in-situ concurrent spectral and depth data collected over a supraglacial lake in West Greenland by means of instruments mounted on a remotely controlled boat. We analyze the spatial distribution of *Ad* to assess the hypothesis of its spatial uniformity and compare *Ad* mean values with those obtained from shallow waters at the lake edge. We also study the spectral dependency of both *Ad* and *g* obtained from in-situ measurements and compare their values against those obtained using literature approaches. This analysis is extended to satellite measurements for the estimates of lake depth from either the LANDSAT and MODIS sensors with those obtained in-situ, quantifying the uncertainty of current procedures for multispectral bathymetry of supraglacial lakes.

2 Supraglacial lake bathymetry from visible data

In the following, we briefly summarize the equations used for estimating lake depth from visible data, together with the hypotheses behind the retrieval scheme.

The expression for reflectance immediately below the water surface for optically shallow, homogeneous water is given by Philpot (1989):

$$R(0^-) = R_\infty + (Ad - R_\infty)\exp(-gz) \quad (1)$$

where *Ad* is the irradiance reflectance (albedo) of the bottom, $Ad = Eu(z)/Ed(z)$, with *Eu* being the upwelling irradiance and *Ed* the downwelling irradiance at depth z, and R_∞ is the irradiance reflectance of an optically deep water column. Resolving Eq. (1) for z gives:

$$z = -(\ln(Ad - R_\infty) - \ln(R(0)^- - R_\infty))/g \quad (2)$$

The coefficient g accounts for losses in both the upward and downward directions and is given by $g \approx Kd + aDu$ (Philpot, 1989), where *Kd* is the diffuse attenuation coefficient

TCD
5, 479–498, 2011

for downwelling light, a is the beam absorption coefficient, and Du is an upwelling light distribution function or the reciprocal of the upwelling average cosine (Mobley, 2004). According to Philpot (1989), the two attenuation coefficients g and Kd are spectrally similar as long as the diffuse attenuation is not dominated by scattering. However, Kd and g cannot be used interchangeably and a possible range of $1.5\,Kd < g < 3\,Kd$ can be assumed in the case of strongly absorbing waters. Philpot (1989) approximates $g \approx 2\,Kd$, for purposes of computation (Table 1, Philpot, 1989). In this study, we use the values of the diffuse attenuation coefficient Kd of optically pure water as reported in Smith and Baker (1981).

3 The remotely controlled boat and the instruments

A commercially sold remotely controlled boat (http://www.viperfishing.co.uk/, Fig. 1) was customized and equipped with a GPS/sonar (HDS-5 Lowrance), an above-surface irradiance sensor for incoming solar radiation, a below-surface downward looking radiance sensor, a spectrometer (Ocean Optics) and a micro computer (used to synchronize the data from the different instruments). The boat is made of glossy acrylic capped ABS and propelled by dual jet-pump engines. It is designed to carry loads up to 6 kg and is controlled remotely with a range up to 1000 m, making it ideal for our application. The original design of the boat was altered to accommodate our needs and specific parts of the watercraft were machined at our laboratory. The decision to use a remotely controlled boat, as opposed to a manned watercraft, aimed to eliminate life-threatening risks associated with a possible rapid drainage of the lake (e.g., Das et al., 2008).

The boat was deployed on 2, 3 and 5 July 2010, on the west margin of the GrIS (Lake Olivia, 69°36′35″ N, 49°29′40″ W), with deployment time usually occurring when the sun was at the zenith and measurements lasting for a few hours. As the boat average speed was $1\,m\,s^{-1}$ and the GPS data were recorded every second, we estimate a spatial resolution of 1 m for the in-situ data. The total number of samples used in

TCD
5, 479–498, 2011

our analysis is ∼6000. The spectral (450–1050 nm, with a 0.3 nm resolution) and depth data collected between two subsequent GPS acquisitions were averaged and assigned to the first of the two GPS locations. The irradiance and radiance sensors were cross-calibrated in the laboratory following Mueller (2003). The diffuse irradiance leaving the outlet of an integrating sphere, illuminated by a calibrated xenon lamp, was measured by the irradiance sensor directed at the outlet. Radiance measurements were then taken of a Spectralon© target (99%) put in place of the irradiance sensor. These measurements were used to derive reflectance from irradiance and radiance intensity measurements and cross-calibrate the two sensors. Though spectral data was collected up to 1050 nm, we focus our analysis on the 450–650 nm range, because of the reduced sensitivity to lake depth above 650 nm. Measurements for lake depth values less than 1 m are excluded from our analysis because of the relatively small sensitivity of the reflectance data in the LANDSAT and MODIS blue and green bands to shallow waters.

4 Analysis of in-situ data

The boat paths, and the corresponding measured depth, are superimposed on a high-resolution (0.5 m) image collected on 4 July 2010 by the WorldView-2 sensor (http://worldview2.digitalglobe.com/, Fig. 2). Shallow waters are located along the edge of the lake, with depth increasing toward its center, up to ∼4.5 m. In Fig. 3 we plot the in-situ water-leaving reflectance spectrally averaged over the LANDSAT band 1 ($B1_{LANDSAT}$, 450–515 nm), band 2 ($B2_{LANDSAT}$, 525–605 nm) and band 3 ($B3_{LANDSAT}$, 630–690 nm) vs. the in-situ measured lake depth. In-situ measured water-leaving reflectance is fitted with Eq. (1), using Ad, g and R_∞ as free fitting parameters. The values obtained for g are: $g_{B1\_LANDSAT\_fit} = 0.023\,m^{-1}$, $g_{B2\_LANDSAT\_fit} = 0.24\,m^{-1}$ and $g_{B3\_LANDSAT\_fit} = 0.81\,m^{-1}$. The corresponding g values obtained assuming $g = 2\,Kd$ (with Kd obtained from Smith and Baker (1981)) are $g_{B1\_LANDSAT\_2Kd} = 0.045\,m^{-1}$,

TCD
5, 479–498, 2011

$g_{B2\_LANDSAT\_2Kd} = 0.21\,m^{-1}$ and $g_{B3\_LANDSAT\_2Kd} = 0.65\,m^{-1}$. The fitted values of g are consistent with those computed assuming $g = 2\,Kd$, though differences exist.

To better understand these differences, we analyzed the spectral dependency of the bottom albedo Ad and coefficient α. Figures 4a and b show, respectively, the values of $\alpha\,g$ (Fig. 4a) and Ad (Fig. 4b) in the 450–650 nm region obtained by minimizing the difference between measured water-leaving reflectance values and those simulated using Eq. (1), with α, Ad and R_∞ as free fitting parameters and z measured in-situ. For convenience, the values for R_∞ are incorporated in Fig. 4c, though this parameter is excluded from our analysis. The fitting iterative procedure terminates when the difference between measured and simulated water leaving reflectance, ΔR, is smaller than a threshold value ΔR_T. The sensitivity of the fitting procedure to the choice of ΔR_T is shown Fig. 4, where bars represent the range of the fitted coefficients when ΔR_T is set to 0.01, 0.025, 0.05 and 0.1. The spectrally averaged values for α for the LANDSAT bands 1 and 2 and the spectrally similar MODIS bands 3 and 4 are, respectively: $\alpha_{B1\_LANDSAT} = 1.91$, $\alpha_{B2\_LANDSAT} = 2.33$, $\alpha_{B3\_MODIS} = 1.73$, $\alpha_{B4\_MODIS} = 2.4$. For the lake under study, the optimal (fitted) values for α differ by $\sim +15\%$ (-15%) from the constant value of $\alpha = 2$. An error of 15% on α translates into a lake depth retrieval error of $\sim 17\%$ when using the LANDSAT band 2. Figure 4 also suggests that α increases with wavelength, which cannot be easily explained, aside from a possible chlorophyll concentration in the water, currently considered to be unlikely. A possible explanation is a higher variability of lake-bottom albedo in the blue region, producing a higher degree of uncertainty in our approximated α in that range.

The fitted values of Ad are greater at shorter wavelength and decrease with increasing wavelength, displaying a spectral behavior similar to that of glacier ice albedo (e.g., Grenfell and Perovich, 2004). To evaluate the assumption of estimating the value of Ad from the reflectance of shallow waters, we use data collected by LANDSAT over Lake Olivia on 9 July 2010 (http://glovis.usgs.gov), converted into planetary reflectance following Chander et al. (2009). Though LANDSAT and in-situ data were not collected on the same day, we assume that the lake depth did not change considerably between

TCD
5, 479–498, 2011

6 July and 9 July. This is supported by the small depth change (< 0.2 m) recorded by a pressure transducer positioned into the lake during the period 1 July–6 July and by the analysis of daily WorldView-2 images collected between 4 July and 9 July. Figure 5 illustrates the distribution of *Ad* for the LANDSAT band 1 (black lines) and band 2 (gray lines) obtained resolving Eq. (2) for *Ad*, with *z* obtained from in-situ measurements and R_∞ from the LANDSAT image where deep water ($z > 40$ m) is present (e.g., Sneed and Hamilton, 2007). The distributions of the reflectance values at the two bands estimated from pixels along the lake edge are also plotted. The mean *Ad* values obtained from solving Eq. (2) are $Ad_{\text{LANDSAT\_B1}} = 0.38 \pm 0.013$ and $Ad_{\text{LANDSAT\_B2}} = 0.31 \pm 0.027$; the mean reflectance values for pixels along the lake edge are $R_{\text{Edge\_B1}} = 0.42 \pm 0.058$ for band 1 and $R_{\text{Edge\_B2}} = 0.34 \pm 0.062$ for band 2. The percentage error between the mean *Ad* value and the mean of the reflectance values along the lake edge is 10.5% (8.9%) in the case of the blue (green) LANDSAT band. From Eq. (2), this translates into an average error on lake depth retrieval of −11.8% (−15.9%) when using the LANDSAT band 1 (band 2). The error on depth is maximum for shallow waters with an underestimation down to −23.7 % (−42.7%) and reduces to −4.6% (−4.7%) for lake depth values up to 10 m.

5 Assessment of lake depth from satellite data

Here we compare the lake depth values estimated with LANDSAT and MODIS with those measured in-situ.

Table 1 reports the mean, standard deviation and maximum values of lake depth obtained from satellite data, together with the root mean square error, the mean absolute error, correlation and percentage error between spaceborne-estimated lake depth using either LANDSAT and 500 m MODIS reflectance product (http://modis.gsfc.nasa.gov/data/dataprod/dataproducts.php?MOD_NUMBER=09) and the values measured by the sonar. Results obtained from MODIS are averaged over the period 2 July–5 July 2010, when in situ data were collected. Results obtained when using either

TCD
5, 479–498, 2011

$\alpha = 2$ or the values of α obtained from the fitting procedure above described (Fig. 4b) are reported. The values of the bottom albedo *Ad* are obtained from the mean of the reflectance of shallow waters on the edge of the lake (e.g., Sneed and Hamilton, 2007). As a reference, the mean, standard deviation and maximum depth of the lake depth values measured by the sonar are also shown in the first row of the table. Results indicate that the use of the LANDSAT band 1 tends to overestimate lake depth, with an RMSE ranging between 2.7 and 3 m, a maximum lake depth on the order of 8 m (against the value of 4.55 m measured in situ) and a mean value of ~ 5.5 m. Lake depth is also overestimated when using the MODIS band 3, that is spectrally similar to the LANDSAT band 1. Maximum depth values from MODIS are close to those estimated by LANDSAT band 1 but the mean values from MODIS are higher than those obtained with LANDSAT. Results improve when using either the LANDSAT band 2 or MODIS band 4, with mean depth values ranging between 0.71 m (AQUA) and 3.34 m (LANDSAT). Best results are obtained with LANDSAT when using $\alpha = 2.33$ (from fitting). In this case, mean, standard deviation and maximum depth provide the closest estimates to the measured ones, with a RMSE of 0.45 m. MODIS band 4 tends to underestimate lake depth with respect to in-situ data. In the case of MODIS, the use of the α fitted value deteriorates the performance of the remote sensing algorithm, further reducing the values of the estimated lake depths.

In Table 2 we report the results of our analysis aimed at quantifying the error on lake depth retrieval from the assumptions of a uniform *Ad* value for the whole lake and using the reflectance values of the pixels at the edge of the lake for *Ad*. Lake depth values are estimated using Eq. (2), with *Ad* values given by the mean of the distributions of the bottom albedo values obtained form the concurrent analysis of surface and satellite data or by the mean of the reflectance values along the lake edge. The table includes the mean, standard deviation, maximum value of lake depth obtained from the satellite data together with the root mean square error, the mean absolute error, correlation and percentage error between the lake depth values estimated with the different configurations and the values measured by the sonar. Results from both

TCD
5, 479–498, 2011

LANDSAT (bands 1 and 2) and MODIS (bands 3 and 4) are reported. In general, best results are obtained when using the LANDSAT band 2 when *Ad* is given by the mean of the *Ad* distribution computed from the conjunct analysis of satellite and surface data (with a RMSE of 0.7 m and a percentage absolute error of ∼35%). Depth estimates using LANDSAT band 1 show a larger standard deviation and higher maximum depth values (above the maximum measured depth), likely as a consequence of the smaller diffuse attenuation coefficient in the blue band (Smith and Baker, 1980). Maximum lake depth values estimated when using LANDSAT band 2 are closer to the value measured in situ. The MODIS sensor on TERRA provides smaller lake depth values than those obtained with the one mounted on AQUA. Given the short time-series it is not possible to assess whether this is a consistent factor and what are the causes. The values estimated by MODIS on TERRA are the closest to those estimated by LANDSAT and measured in situ. Lake depth values estimated from MODIS when using band 4 are generally smaller than those measured in situ.

6 Conclusions and future work

We collected in-situ concurrent multi-spectral and depth observations over a supraglacial lake in Greenland in order to assess spaceborne bathymetry. Such measurements allowed us to study the spectral dependency of the bottom albedo *Ad* and coefficient α with the latter linearly relating the attenuation cofficient g and the diffuse attenuation factor *Kd*. Results show that, as expected, the spectral behavior of *Ad* is similar to that of glacier ice albedo. The increase of α with wavelength from in-situ data cannot be easily explained without assuming chlorophyll in the water, which is present in a minimal concentration according to our preliminary analysis of water samples. One explanation for the spectral behavior of α is that the bottom albedo has a higher variability in the blue region, attributing some of the loss due to a darker blue ice to loss along the water column.

TCD
5, 479–498, 2011

We assessed a widely used literature technique in which *Ad* is assumed to be uniform and equal to the reflectance of shallow waters along the lake edge. The analysis of in-situ measurements show a Gaussian-like behavior of *Ad*, with this variability appearing to be intrinsic to the albedo of the bottom, consisting of large patches of atmospherically transported material. The difference between the mean *Ad* value obtained from in-situ measurements and the mean of the reflectance values along the lake edge obtained from LANDSAT is on the order of $\sim 10\%$. This translates into an average error on lake depth retrieval of -11.8% (-15.9%) when using the LANDSAT band 1 (band 2). The error is maximum for shallow waters with an underestimation down to -23.7% (-42.7%) and reduces to -4.6% (-4.7%) for lake depth values up to 10 m.

In the case of α, the values obtained from in-situ measurements differ by $\sim 15\%$ from those computed using literature approaches. Best spaceborne-based estimates were obtained when using either the LANDSAT band 2 or the spectrally similar MODIS band 4. In the case of LANDSAT, best results are obtained when using the α value derived from in-situ measurements ($\alpha = 2.33$). However, this is not true in the case of MODIS, where best results are obtained using the values suggested in the literature ($\alpha = 2$). In the case of MODIS, however, mixed-pixel effects and relatively coarse resolution can be responsible for large uncertainty. For example, the presence of ice within a pixel will increase the reflectance with respect to a pixel containing only liquid water, leading to an underestimation of the lake depth. This is especially true for relatively small lakes and for those pixels containing the lake edges.

We plan to collect a more comprehensive in-situ data set on the inherent optical properties of melt pond water and to extend our analysis to multiple lakes. We also plan to use a more sophisticated model of the water column (Lee, 1999), where depth estimations can be made with a fully physical model of water constituents.

Acknowledgements. This work was supported by the NSF grant ANS 0909388, by the NASA Cryosphere Program and by the World Wildlife Foundation (WWF).

TCD
5, 479–498, 2011

References

Box, J. E. and Ski, K.: Remote sounding of Greenland supra-glacial melt lakes: implications to sub-glacial hydraulics, J. Glaciol., 181, 257–265, 2007.

Chander, G., Markham, B. L., and Helder, D. L.: Summary of current radiometric calibration coefficients for Landsat MSS, TM, ETM+, and EO-1 ALI sensors, Remote Sens. Environ., 113, 893–903, 2009.

Das, S. B., Joughin, I., Behn, M. D., Howat, I. M., King, M. A., Lizarralde, D., and Bhatia, M. P.: Fracture propagation to the base of the Greenland ice sheet during supraglacial lake drainage, Science, 320, 778–781, 2008.

Georgiu, S., Shepherd, A., McMillan, M., and Nienow, P.: Seasonal evolution of supraglacial lake volume from ASTER imagery, Ann. Glaciol., 50(52), 95–100, 2009.

Grenfell, T. C. and Perovich, D. K.: Seasonal and spatial evolution of albedo in a snow-ice-land-ocean environment, J. Geophys. Res., 109, C01001, doi:10.1029/2003JC001866, 2004.

Joughin, I., Tulaczyk, S., Fahnestock, M., and Kwok, R.: A mini-surge on the Ryder Glacier, Greenland, observed by satellite radar interferometry, Science, 274, 228–230, 1996.

Lee, Z., Carder, K. L., Mobley, C. D., Steward, R. G., and Patch, J. S.: Hyperspectral remote sensing for shallow waters. 2. Deriving bottom depths and water properties by optimization, Appl. Optics, 38(18), 3831–3843, 1999.

Lüthje, M., Pedersen, L. T., Reeh, N., and Greuell, W.: Modelling the evolution of supra-glacial lakes on the West Greenland ice-sheet margin, J. Glaciol., 52, 608–618, 2006.

Maritorena, S., Morel, A., and Gentili, B.: Diffuse reflectance of oceanic shallow waters: Influence of water depth and bottom albedo, Limnol. Oceanogr., 39(7), 1689–1703, 1994.

McMillan, M., Nienow, P., Shepherd, A., Benham, T., and Sole, A.: Seasonal evolution of supra-glacial lakes on the Greenland ice sheet, Earth Planet. Sc. Lett., 262, 484–492, 2007.

Mobley, C. D.: Estimation of the remote-sensing reflectance from above-surface measurements, Appl. Optics, 38(36), 7442–7455, 1997.

Mueller, J.: In-Water Radiometric Profile Measurements and Data Analysis Protocols, NASA/TM-2003-21621/Rev-Vol III, 7, 2003.

Mueller, J., McClain, G., Bidigare, R., Trees, C., Balch, W., Dore, J., Drapeau, D., Karl, D., and Van, L. : Ocean optics protocols for satellite ocean color sensor validation, revision 5, Vol. V, Biogeochemical and bio-optical measurements and data analysis protocols, NASA Tech. Memo., 2003-211621, Rev, 5, 2003.

TCD
5, 479–498, 2011

Philpot, W. D.: Bathymetric mapping with passive multispectral imagery, Appl. Optics, 28(8), 1569–1578, 1989.

Smith, R. C. and Baker, K. S.: Optical properties of the clearest natural waters (200–800 nm), Appl. Optics, 20, 2, 177–1846, 1981.

Sneed, W. A. and Hamilton, G. S.: Evolution of melt pond volume on the surface of the Greenland Ice Sheet, Geophys. Res. Lett., 34, L03501, doi:10.1029/2006GL028697, 2007.

Sundal, A. V., Shepherd, A., Nienow, P., Hanna, E., Palmer, S., Huybrechts, P.: Evolution of supra-glacial lakes across the Greenland Ice Sheet, Remote Sens. Environ., 113, 2164–2171, 2009.

Pimentel, S. and Flowers, G. E.: A numerical study of hydrologically driven glacier dynamics and subglacial flooding, Proc. R. Soc. A., 467, 537–558, doi:10.1098/rspa.2010.0211, 2010

TCD
5, 479–498, 2011

Table 1. Statistics on lake depth retrieval using different space-borne sensors, bands and hypotheses on the value of the α coefficient.

	Mean [m]	Std. dev. [m]	Max. [m]	RMSE [m]	Correlation
SONAR	2.83	0.97	4.55	n/a	n/a
LANDSAT BAND 1 (450–515 nm)					
$\alpha = 2$	5.53	1.53	8.01	2.71	0.79
$\alpha = 1.91$	5.79	1.6	8.44	2.97	0.78
LANDSAT BAND 2 (525–605 nm)					
$\alpha = 2$	3.34	0.91	4.72	0.59	0.84
$\alpha = 2.33$	2.86	0.78	4.05	0.45	0.85
MODIS TERRA (AQUA) – BAND 3 (459–479 nm)					
$\alpha = 2$	6.5 (2.3)	1.93 (1.47)	8.65 (4.14)	n/a	n/a
$\alpha = 1.91$	6.93 (2.44)	2.04 (1.56)	9.18 (4.39)	n/a	n/a
MODIS TERRA (AQUA) – BAND 4 (545–565 nm)					
$\alpha = 2$	2.1 (0.9)	0.92 (0.9)	2.9 (1.9)	n/a	n/a
$\alpha = 2.33$	1.71 (0.71)	0.75 (0.74)	2.44 (1.56)	n/a	n/a

TCD
5, 479–498, 2011

Table 2. Statistics on lake depth retrieval using different sensors, bands and hypothesis on the bottom albedo values *Ad*.

	Mean [m]	Std. dev. [m]	Max. [m]	RMSE [m]	MAE [m]	Correlation	% absolute error
			SONAR				
	2.83	0.97	4.55	n/a	n/a	n/a	n/a
			LANDSAT				
			BAND 1 (450–515 nm)				
$Ad = \mu_{AdLANDSAT\_B1}$	2.86	1.53	5.39	0.97	0.69	0.79	1.29
$Ad = \mu_{Edge\_B1}$	5.71	1.52	8.25	3.04	2.9	0.78	112.9
			BAND 2 (525–605 nm)				
$Ad = \mu_{AdLANDSAT\_B2}$	2.85	0.91	4.24	0.53	0.44	0.84	1.12
$Ad = \mu_{Edge\_B2}$	3.28	0.9	4.67	0.7	0.55	0.85	13.83
			MODIS				
			BAND 3 (459–479 nm)				
TERRA (2 July–5 July)	6.5	1.93	8.65	n/a	n/a	n/a	n/a
AQUA (2 July–5 July)	2.3	1.47	4.14	n/a	n/a	n/a	n/a
			BAND 4 (545–565 nm)				
TERRA (2 July–5 July)	2.1	0.92	2.9	n/a	n/a	n/a	n/a
AQUA (2 July–5 July)	0.9	0.9	1.9	n/a	n/a	n/a	n/a

TCD
5, 479–498, 2011

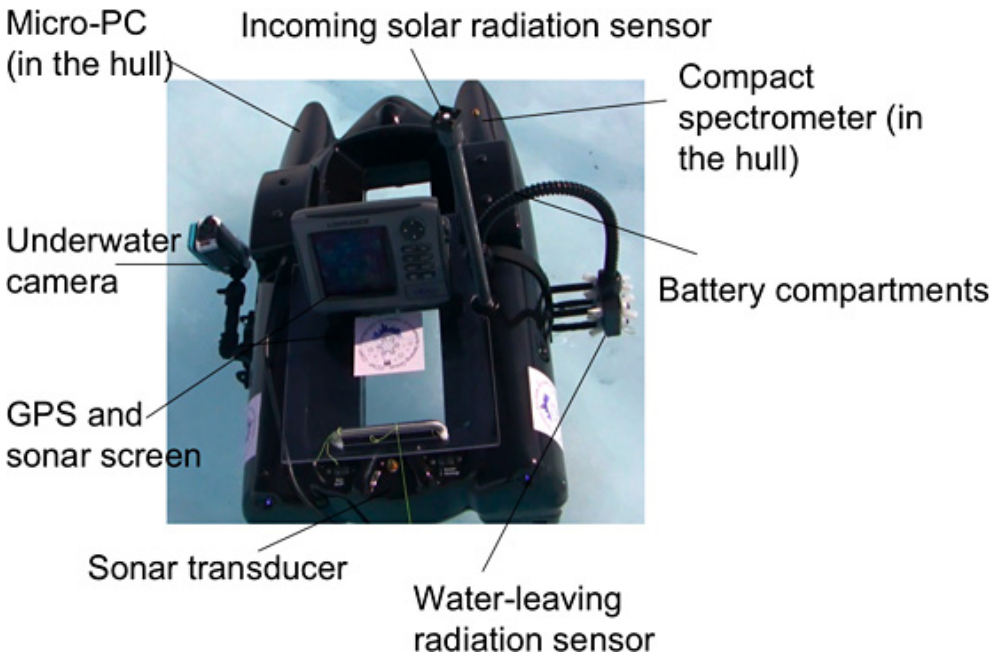

Fig. 1. The customized remotely controlled boat with the different instruments.

TCD
5, 479–498, 2011

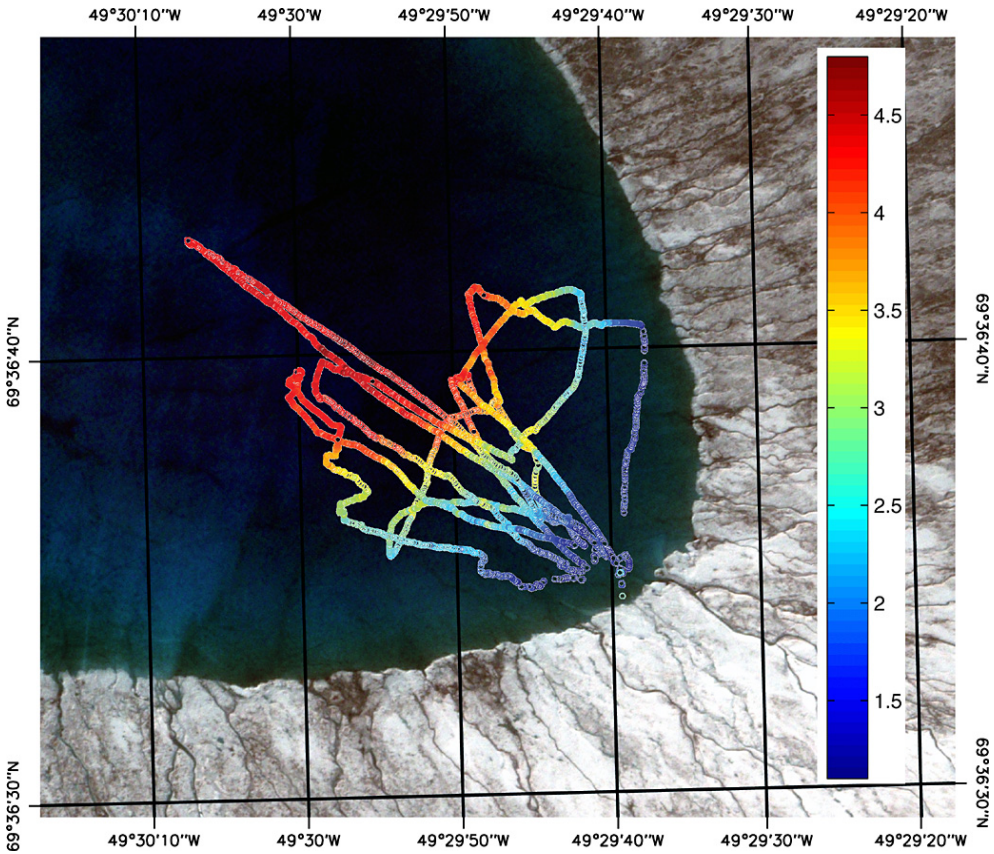

Fig. 2. Boat paths and measured depth values imposed over a high-resolution (0.5 m) Worldview-2 image.

TCD
5, 479–498, 2011

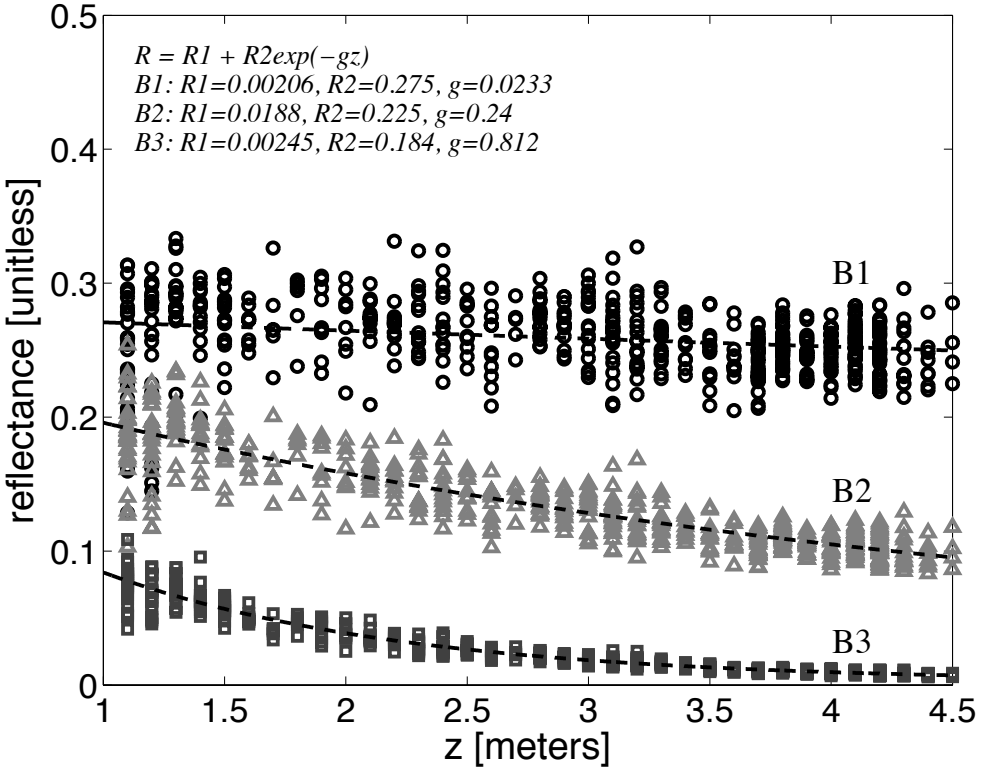

Fig. 3. In-situ measured water-leaving reflectance values vs. lake depth for the LANDSAT bands 1, 2 and 3 and exponential fitting.

TCD
5, 479–498, 2011

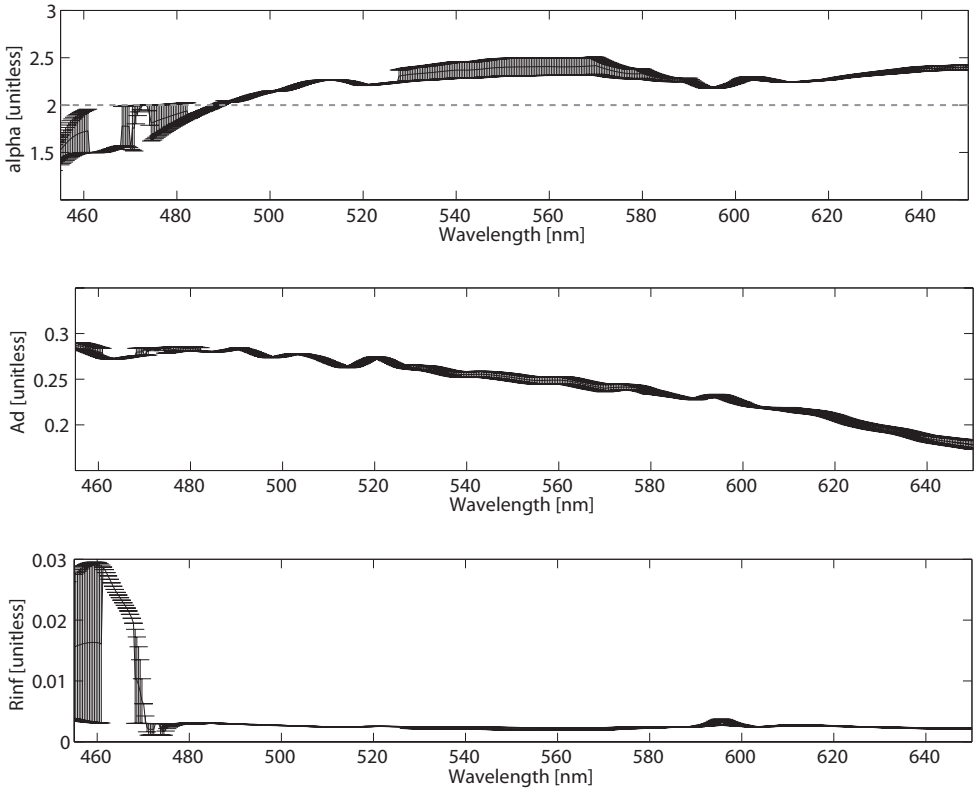

Fig. 4. Spectral dependency of α (top) and Ad (bottom) values derived from the minimization of the difference ΔR between measured and theoretical water-leaving reflectance values. Bars represent the range of values when different ΔR values are used (see text for details).

TCD
5, 479–498, 2011

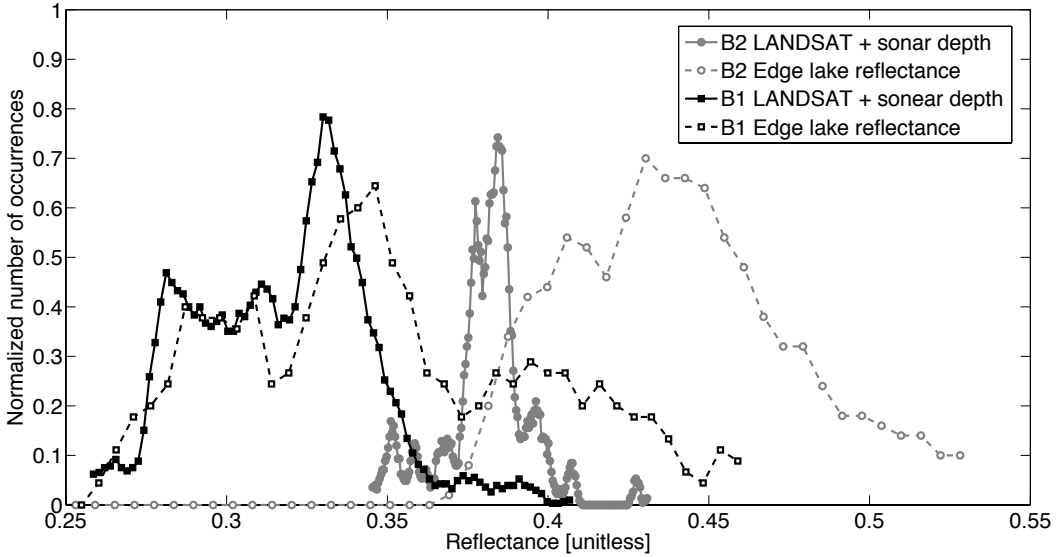

Fig. 5. Distribution of *Ad* values for the LANDSAT bands 1 and 2 estimated from Eq. (2) using lake depth measured by the boat (cont. lines) and of reflectance values from the edge lake (dashed lines).

TCD
5, 479–498, 2011